Measuring Topological Invariants in Photonic Systems

Mohammad Hafezi
Joint Quantum Institute, NIST/University of Maryland, College Park, Maryland 20742, USA
(Received 5 December 2013; published 29 May 2014)

Motivated by the recent theoretical and experimental progress in implementing topological orders with photons, we analyze photonic systems with different topologies and present a scheme to probe their topological features. Specifically, we propose a scheme to modify the boundary phases to manipulate edge state dynamics. Such a scheme allows one to measure the winding number of the edge states. Furthermore, we discuss the effect of loss and disorder on the validity of our approach.

DOI: 10.1103/PhysRevLett.112.210405 PACS numbers: 03.65.Vf, 42.25.-p, 73.43.Cd

Topology plays a fundamental role in many physical phenomena in two-dimensional systems. The most famous examples are various quantum Hall effects in electronic systems [1–3]. Recently, there has been a surge of interest in studying topological orders in nonelectronic systems, ranging from ultra cold atoms [4–7] to photons [8–20]. For example, it was shown that a uniform magnetic field can be synthesized in an array of coupled resonators and the system exhibits chiral edge states, in direct analogy to integer quantum Hall edge states [13]. The robustness of such edge states against disorder was experimentally confirmed by direct imaging of the photonic array.

While the implementation of gauge fields has been achieved, the measurement of the expected topological orders remains elusive due to the inapplicability of the conventional Hall conductance measurements to atomic and photonic systems. There have been various proposals to detect topological order in atomic [21–26] and, recently, photonic systems [27,28], which are generally based on the manipulation of Bloch states. However, the following question has not yet been addressed: how can one directly measure the integer topological invariants, e.g., the winding number of the edge states or the Chern number of the bulk state in a photonic system? In particular, how do the integer values manifest themselves in an optical realization of quantum Hall Hamiltonians. In this Letter, we propose a scheme to measure the integer topological invariants of a photonic system by manipulating the boundary conditions. Following Refs. [12,13], we benefit from individual site addressability to manipulate the synthetic gauge field at the boundary—a property which is difficult to achieve in electronic and atomic systems.

The main idea of our approach relies on the ability to introduce a nonzero phase in the boundary conditions. Such a phase is equivalent to a magnetic flux threading the holes of the system when the system manifold is not simply connected. If the system has an edge state around that hole, the insertion of the magnetic flux shifts the momentum of that edge state. Once an entire magnetic flux quantum threads the hole, the edge state spectrum should return to its original form, while an integer number of edge states have been transferred during this process (Fig. 1). This integer number is the winding number of the edge state. We propose that, in a photonic implementation, such a spectral shift and edge state transfer can be experimentally observed using standard transmission spectroscopy. We note that our proposal could be applied to all topologically ordered photonic systems, ranging from radio frequency [29] and microwave [30] to an optical domain, and any bosonic system that can be externally driven. In particular, in circuit-QED systems, whispering gallery mode resonators [31], and in exciton-polariton systems, micropillars [32] can be used to make an array of resonators, respectively.

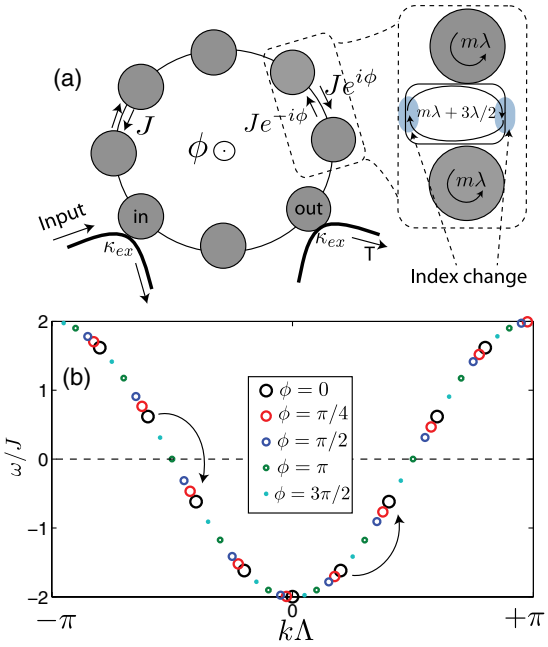

FIG. 1 (color online). (a) Coupled resonators in a ring configuration: Photons hop between resonators with the rate J, except for one link where they hop with $Je^{i\phi}$. The inset shows that the boundary can be modified by changing the index of refraction of the connecting resonators. (b) Dispersion relation when the boundary phase changes from zero to 2π, for a ring of 10 resonators.

For concreteness, we discuss the optical scheme based on a platform proposed in Ref. [12] and recently implemented in Ref. [13] using silicon-on-insulator technology. Before presenting the scheme to measure the integer topological invariants in a 2D system, we present the case of a trivial topology, i.e., the ring, to clarify the spectral dynamics in the presence of a threading flux.

Ring.—We consider an array of N coupled resonators that form a ring and study the effect of a synthetic magnetic flux threading the ring, as shown in Fig. 1. The Hamiltonian of the system is given by

$$H_{\text{ring}} = -J\sum_{i=1}^{N-1}\hat{a}_i^\dagger\hat{a}_{i+1} + \text{H.c.}, \tag{1}$$

where J is the tunneling rate between two sites and $\hat{a}_i^\dagger$ is the creation operator at the site i. The Hamiltonian terms that describe the coupling between the first and the last site are $-J\hat{a}_1^\dagger\hat{a}_N e^{i\phi} + \text{H.c.}$, where ϕ is the tunneling phase. In other words, the twist angle in the generalized boundary condition can be generated by such a term in the system Hamiltonian. For charged particles, this phase can be obtained by introducing a magnetic flux in the middle of the ring, whereas in our system, this phase has to be artificially engineered. Note that such a phase does not have to be local on the last link; i.e., it can be distributed around the ring and generate the same effect.

Following Ref. [12], the tunneling with a hopping phase between the resonators can be induced by connecting resonators that are antiresonant with the primary resonators, as shown in the inset of Fig. 1. Specifically, we assume that the perimeter of the primary resonators is $m\lambda$ where m is an integer and λ is the resonant wavelength. If the perimeter of the connecting resonators is chosen to be $m\lambda + 3\lambda/2$, i.e., antiresonant with the primary resonators, it will induce a coupling between the two primary resonators described by the Hamiltonian: $-J\hat{a}_i^\dagger\hat{a}_j + \text{H.c.}$ Now, the tunneling term can take a phase if the optical paths for the forward and backward hopping are different. In Refs. [12,13], this was achieved by having a passive length imbalance between the connecting paths. Similarly, if the index of refraction of the upper and lower arms is changed with opposite signs, so that the overall connecting resonator remains antiresonant with the primary resonators, the forward and backward hopping acquires opposite phases, described by the Hamiltonian: $-J\hat{a}_i^\dagger\hat{a}_j e^{i\phi} + \text{H.c.}$ Specifically, the hopping phase is equal to $\phi = 2\pi\Delta x/\lambda$, where Δx is the difference between the optical path lengths in the connecting resonators. Such an index change can be achieved through an optical [33] or electrical [34] carrier injection or thermal tuning [35]. Alternatively, a nonreciprocal phase can be induced by modulating the connecting waveguides [36] or using optomechanics [11]. Regardless of the experimental scheme, the dispersion relation of the ring is $\omega = -2J\cos(k\Lambda + \phi/N)$.

Note that the phase is divided by N since the hopping phase is introduced only at one link and it does not depend on how the phase is distributed over the lattice, as long as the total hopping phase is equal to ϕ. In the context of the conventional tight-binding model, k can be interpreted as the Bloch wave number and Λ as the lattice spacing. Here, $k\Lambda$ is simply the phase difference between two adjacent resonators. In a finite system, the eigenenergies are positioned on a finite number of points on the same dispersion curve, as shown in Fig. 1(b). Changing the twist angle ϕ shifts the energy spectrum in one direction, along the dispersion curve. When one flux quantum is inserted ($\phi = 0 \to 2\pi$), the momentum of each energy state moves by $2\pi/N$ and each state replaces the adjacent state in the Brillouin zone, as shown in Fig. 1(b).

In a photonic system, such a state transfer can be probed through transmission spectroscopy. Using the input-output formalism [37], the field dynamics of the resonators is given by

$$\dot{\hat{a}}_j = i[H, \hat{a}_j] - (\delta_{j,\text{in}} + \delta_{j,\text{out}})\kappa_{ex}\hat{a}_j - \delta_{j,\text{in}}\sqrt{2\kappa_{ex}}\mathcal{E}_{\text{in}}e^{-i\omega t}, \tag{2}$$

where κ_{ex} is the extrinsic coupling rate between the probing waveguide and the resonators. The indices "in" ("out") represent the resonators to which the input (output) probing waveguides are connected. In the linear regime where $\langle\hat{a}_i\rangle = a_i$, we can obtain the transmission in the output channel as $T = |a_{\text{out}}/\mathcal{E}_{\text{in}}|^2$, where $\mathcal{E}_{\text{in}}$ is the input field. Figure 2 shows the transmission spectrum of the system when the array is probed using an input and output waveguide [shown in Fig. 1(a)]. Since the input and output waveguides are coupled to single sites, the incoming photon is coupled to all momenta and the transmission spectrum only resolves the energy and not the momentum of system eigenstates.

In the absence of the magnetic flux ($\phi = 0$), the spectrum is twofold degenerate, which corresponds to Bloch waves going clockwise and counterclockwise around the ring. However, in the presence of the magnetic flux ($\phi \neq 0$), the spectrum is not necessarily degenerate, and therefore, all the states can be resolved using transmission spectroscopy in the undercoupled limit ($\kappa_{ex} < 4J/N$); i.e., the finite size

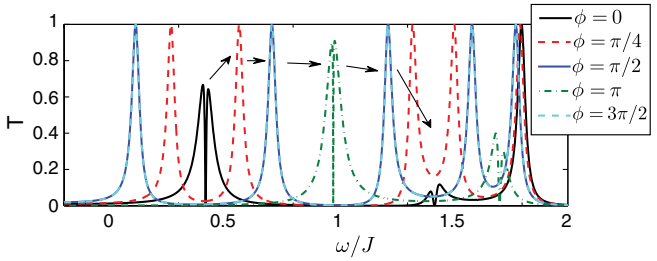

FIG. 2 (color online). Probing the state transfer in a ring using transmission spectroscopy. The simulation is performed for 10 sites and $\kappa_{ex}/J = 0.1$. The input and output probes are separated by two sites, as shown in Fig. 1(b).

of the system allows us to track the transfer of the states. We readily observe that when $\phi: 0 \to 2\pi$, the transmission spectrum returns to its original profile and each peak moves and replaces its adjacent peak. We use similar tools to investigate a two-dimensional system.

Annulus.—We consider an annulus similar to Laughlin-Halperin's argument [38,39] to study edge state transfer. Specifically, following Hatsugai's work [40], we consider a 2D lattice with a uniform perpendicular magnetic field, where the Hamiltonian of the system is given by

$$H_{\mathrm{mag}} = -J\sum_{x,y} \hat{a}^{\dagger}_{x+1,y}\hat{a}_{x,y}e^{i2\pi\alpha y} + \hat{a}^{\dagger}_{x,y}\hat{a}_{x+1,y}e^{-i2\pi\alpha y} + \hat{a}^{\dagger}_{x,y+1}\hat{a}_{x,y} + \hat{a}^{\dagger}_{x,y}\hat{a}_{x,y+1}, \quad (3)$$

where $\hat{a}^{\dagger}_{x,y}$ is the creation operator at the site (x, y), and α characterizes the phase imbalance. Specifically, a photon hopping around a plaquette, in the clockwise direction, acquires the phase $2\pi\alpha$, in direct analogy to Aharanov-Bohm phase. Therefore, α is the effective magnetic flux per plaquette, and therefore, the total magnetic flux is $N_\alpha = \alpha N_x N_y$. As it was theoretically proposed in Ref. [12] and experimentally demonstrated in Ref. [13], this Hamiltonian can be implemented in an array optical resonators. In particular, such hopping phases can be obtained when the optical paths for the forward and backward hopping are different, as described above (Fig. 1 inset).

For an infinite system, the Hamiltonian of Eq. (2) yields the Hofstadter butterfly spectrum [41]. In particular, when the magnetic flux is rational, $\alpha = p/q$ with mutually prime integers, the system has q distinct (gapped) bands [41]. On a finite annulus, or any other equivalent topology, e.g., a cylinder or a square with a hole in the middle, the system has edge states which are spectrally located between the magnetic bands and are spatially confined at the edges. The dispersion of the edge states is shown in Fig. 3(b). As shown by Hatsugai [40], the winding number of such edge states is related to the Chern number of the bulk states, and is given by the following Diophantine equation [42]:

$$n = s_n q + t_n p, \qquad |t_n| \le q/2, \quad (4)$$

where t_n and s_n are integers and n is the gap index $(1 \le n \le q-1)$, and t_n is the winding number of the nth gap. The Chern number of the nth bulk band is given by $t_n - t_{n-1}$ with $t_0 = 0$.

Besides the overall uniform magnetic flux (α), we assume that the system is threaded with a synthetic magnetic flux ϕ through the hole of the annulus. When the magnetic flux is changed from zero to one quantum, the edge states are transferred [40]. We can easily trace the edge states and count how many of them have been transferred during the insertion of a magnetic flux. By connecting the probing waveguides to the outer (inner) edges, we can selectively couple to the outer (inner) edge states, respectively, as shown in Figs. 3(c)–3(d). In particular, when the connecting waveguides are coupled to the outer (inner) edge of the system, the coupling to the inner (outer) edge is exponentially suppressed as $\exp(-N_y/l_B)$, where $l_B^{-1} = \sqrt{2\pi\alpha}$ is the magnetic length, in units of the lattice spacing. We focus on the third gap, where for a system with $\alpha = 1/4$, the winding number is one ($t_3 = -1$), according to Eq. (4). As shown in Figs. 3(c)–3(d), the edge states are transferred by one peak, in agreement with the value of the winding number, which is one in this case. The case of winding number one is similar to the ring case which was discussed above, where the insertion of a magnetic flux transfers the edge states by one. Such a state transfer is in direct analogy to the electronic case [38–40], where during a flux insertion an integer number of states is transferred above or below the Fermi level; in the photonic case, the frequency of the incoming photons plays the role of the Fermi level, as shown by a dashed line in Figs. 3(c)–(d). Note that the inner and outer edge spectrum move in opposite directions. In general, the number of edge states might be larger than the winding number. Therefore, in transmission spectrum some peaks may move forwards and some backwards. However,

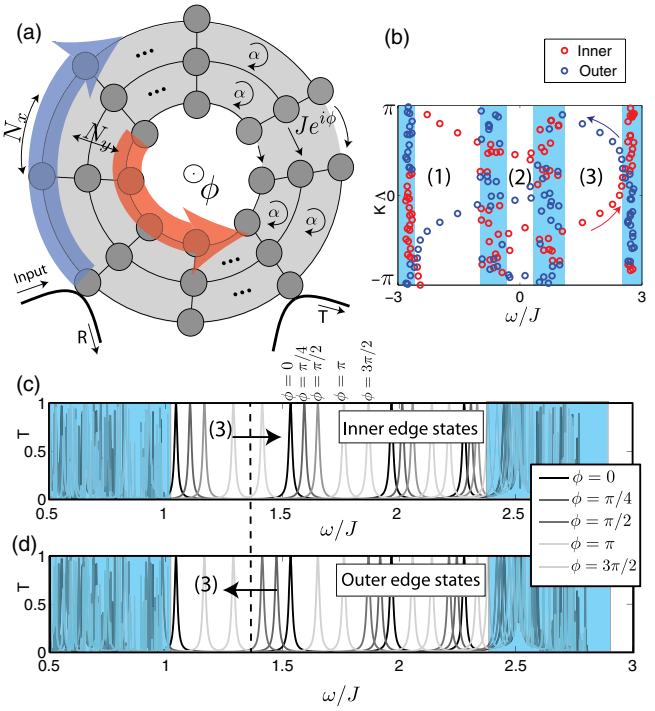

FIG. 3 (color online). (a) Cylinder or annulus topology, the system is under a uniform magnetic flux per plaquette α and the hole is threaded with a magnetic flux ϕ. (b) shows the dispersion relation for $\phi = 0$. The bulk gap indices are shown. (c),(d) The state transfer for inner and outer edges, respectively, where the threading flux is changed from zero to 2π. The simulation is performed for $(N_x, N_y) = (20, 10)$, $\alpha = 1/4$, and $\kappa_{ex}/J = 0.1$. Blue shades represent the bulk states. The dashed lines are guides to the eye to highlight the number of edge states transferred during a single flux insertion.

since the winding number is a topological invariant, the difference between the number of forward and backward going states, at any frequency in the edge band, will be uniquely determined by the winding number.

This scheme can be generalized to probe winding numbers larger than one. Similarly, the insertion of a magnetic flux does not change the eigenstates of the system, and therefore, the transmission spectrum remains intact. Since in the transmission spectroscopy the momentum is not resolved, all the edge state curves in the dispersion relation are projected onto the energy axis. Therefore, at any fixed frequency in the edge band, multiple peaks can pass during a flux insertion. In Fig. 4, we consider the situation where $\alpha = 1/6$. For the fourth gap (i.e., $0.6 \leq \omega/J \leq 1.4$), the winding number is $t_4 = -2$. Therefore, two edge state resonances cross the dashed line. Note that if group velocities of different edge state curves are close to each other, resonances cross one after another [e.g., $0.6 < \omega/J < 1.0$ in Fig. 4(b)]. In contrast, if group velocities are very different than each other, then resonances can cross each other [e.g., $1 < \omega/J < 1.4$ in Fig. 4(b)]. However, in both cases, the number of resonances crossing a fixed frequency line (shown by the dashed line) is equal to the winding number, in this case two. In general, if the winding number of the edge state is t_n, the edge resonances cross t_n times any frequency in the edge band when the twist angle is changed by 2π. Moreover, the moving direction of the peak corresponds to the sign of the winding number of the edge states.

Effect of disorder and loss.—In an experimental realization, photonic systems are impaired by loss and disorders. Therefore, we evaluate the effect of such errors and show that the proposed scheme can still probe the topological invariants. The major source of loss in silicon-on-insulator technology is the propagation loss in silicon resonators, where the guided photons leave the waveguides through elastic scattering [43]. We characterize such loss in our Hamiltonian in the form of $-i\kappa_{\text{in}}\hat{a}_i^\dagger\hat{a}_i$ where κ_{in} is the field intrinsic decay rate to undesired modes. Figure 5(a) shows the effect of such loss on the system of Fig. 2. We observe that the presence of loss decreases the contrast of the transmission spectrum, and as long as the loss rate is at most an order of magnitude lower than the tunneling rate, the transmission peaks are discernible. The other source of error is the frequency mismatch between neighboring resonators. Such disorder is a common problem in integrated photonics [44–46] and can be characterized by a random on-site potential at each site $U_i\hat{a}_i^\dagger\hat{a}_i$ [12]. Figure 5(b) shows the effect of such disorder on the transmission spectrum. The grey area highlights 1 standard deviation from the averaged transmission in the presence of nonmagnetic disorder evaluated for a hundred realizations. As expected from the theory of the integer quantum Hall effect, disorder leads to a broadening of the edge state resonances; however, they are still resolvable, as shown in Fig. 5(b). In contrast, since the bulk states are more susceptible to disorder, the corresponding resonances are washed out, as shown on the left and right of the spectrum. We note that in a physical realization, one may have other types of disorders, such as inhomogeneous tunneling rates and hopping phases (i.e., inhomogeneous magnetic field). However, as long as disorders are weak enough such that the Hofstadter band gaps are not closed, the topological order remains unchanged (see the Supplemental Material [47]).

In conclusion, we have shown that different topologies can be implemented in a photonic system and their integer topological invariants can be measured using standard transmission spectroscopy. The focus of this Letter was the linear regime. Recently, it has been shown that, in the presence of strong optical nonlinearity, an externally driven system can form fractional quantum Hall states, such as Laughlin states [48,49]. An interesting research direction is

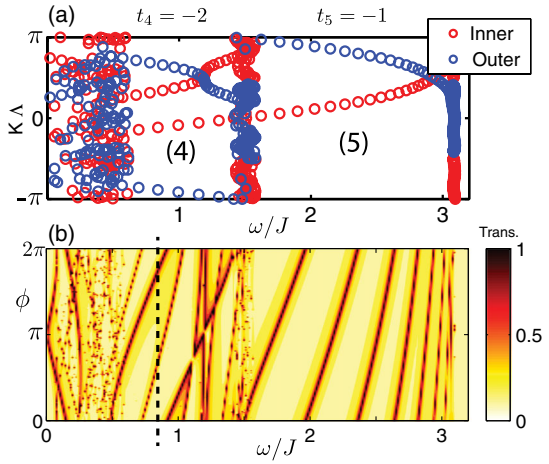

FIG. 4 (color online). (a) Dispersion relation of the fourth and the fifth bands for $\alpha = 1/6$ for a 70×20 lattice. (b) Transmission spectrum as a function of the twist angle ϕ for a 20×14 lattice. The dashed lines are guides to the eye to highlight the number of edge states transferred during a single flux insertion.

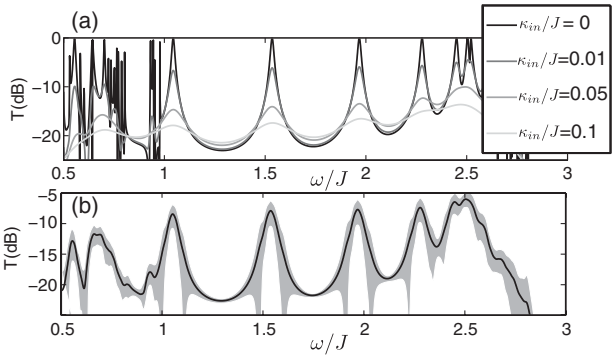

FIG. 5. (a) Transmission spectrum for different values of intrinsic loss $\kappa_{\text{in}}/J = 0$, 0.01, 0.05, 0.1. (b) Transmission spectrum in the presence of intrinsic loss ($\kappa_{\text{in}} = 0.01$) and a Gaussian disorder [$\sigma(U)/J = 0.1$]. All the other parameters are the same as Fig. 3.

to extend these ideas to investigate topological invariants in such driven interacting systems.

We thank Y. Hatsugai, P. Zoller, I. Carusotto, N. Goldman, B. Halperin, J. Taylor, O. Zilberberg, and M. Devoret for fruitful discussions and G. Bryant and J. Peters for their critical reading of the manuscript. This research was supported by the ARO MURI award W911NF0910406, and the NSF through the Physics Frontier Center at the Joint Quantum Institute.

[1] K. V. Klitzing and M. Pepper, Phys. Rev. Lett. **45**, 494 (1980).
[2] D. C. Tsui, H. L. Stormer, and A. C. Gossard, Phys. Rev. Lett. **48**, 1559 (1982).
[3] M. König, S. Wiedmann, C. Brüne, A. Roth, H. Buhmann, L. Molenkamp, X. Qi, and S. Zhang, Science **318**, 766 (2007).
[4] J. Dalibard, F. Gerbier, G. Juzeliūnas, and P. Öhberg, Rev. Mod. Phys. **83**, 1523 (2011).
[5] Y. J. Lin, R. L. Compton, K. Jimenez-Gracia, J. V. Porto, and I. B. Spielman, Nature (London) **462**, 628 (2009).
[6] J. Struck, C. Ölschläger, M. Weinberg, P. Hauke, J. Simonet, A. Eckardt, M. Lewenstein, K. Sengstock, and P. Windpassinger, Phys. Rev. Lett. **108**, 225304 (2012).
[7] M. Aidelsburger, M. Atala, S. Nascimbène, S. Trotzky, Y. A. Chen, and I. Bloch, Phys. Rev. Lett. **107**, 255301 (2011).
[8] F. D. M. Haldane and S. Raghu, Phys. Rev. Lett. **100**, 013904 (2008).
[9] Z. Wang, Y. Chong, J. D. Joannopoulos, and M. Soljacic, Nature (London) **461**, 772 (2009).
[10] R. O. Umucalilar and I. Carusotto, Phys. Rev. A **84**, 043804 (2011).
[11] M. Hafezi and P. Rabl, Opt. Express **20**, 7672 (2012).
[12] M. Hafezi, E. A. Demler, M. D. Lukin, and J. M. Taylor, Nat. Phys. **7**, 907 (2011).
[13] M. Hafezi, S. Mittal, J. Fan, A. Migdall, and J. Taylor, Nat. Photonics **7**, 1001 (2013).
[14] G. Q. Liang and Y. D. Chong, Phys. Rev. Lett. **110**, 203904 (2013).
[15] A. B. Khanikaev, S. H. Mousavi, W. K. Tse, and M. Kargarian, Nat. Mater. **12**, 233 (2012).
[16] K. Fang, Z. Yu, and S. Fan, Nat. Photonics **6**, 782 (2012).
[17] Y. E. Kraus, Y. Lahini, Z. Ringel, M. Verbin, and O. Zilberberg, Phys. Rev. Lett. **109**, 106402 (2012).
[18] M. Verbin, O. Zilberberg, Y. E. Kraus, Y. Lahini, and Y. Silberberg, Phys. Rev. Lett. **110**, 076403 (2013).
[19] M. C. Rechtsman, J. M. Zeuner, A. Tünnermann, S. Nolte, M. Segev, and A. Szameit, Nat. Photonics **7**, 153 (2012).
[20] M. C. Rechtsman, J. M. Zeuner, Y. Plotnik, Y. Lumer, D. Podolsky, F. Dreisow, S. Nolte, M. Segev, and A. Szameit, Nature (London) **496**, 196 (2013).
[21] H. M. Price and N. R. Cooper, Phys. Rev. A **85**, 033620 (2012).
[22] E. Alba, X. Fernandez-Gonzalvo, J. Mur-Petit, J. K. Pachos, and J. J. Garcia-Ripoll, Phys. Rev. Lett. **107**, 235301 (2011).
[23] D. A. Abanin, T. Kitagawa, I. Bloch, and E. Demler, Phys. Rev. Lett. **110**, 165304 (2013).
[24] N. Goldman, J. Beugnon, and F. Gerbier, Phys. Rev. Lett. **108**, 255303 (2012).
[25] X. J. Liu, K. T. Law, T. K. Ng, and P. A. Lee, Phys. Rev. Lett. **111**, 120402 (2013).
[26] A. Dauphin, and N. Goldman, Phys. Rev. Lett. **111**, 135302 (2013).
[27] T. Ozawa and I. Carusotto, Phys. Rev. Lett. **112**, 133902 (2014).
[28] S. Longhi, Opt. Lett. **38**, 3716 (2013).
[29] N. Jia, A. Sommer, D. Schuster, and J. Simon, arXiv:1309.0878.
[30] W. E. Shanks, D. L. Underwood, and A. A. Houck, Nat. Commun. **4**, (2013).
[31] Z. Minev, I. Pop, and M. Devoret, Appl. Phys. Lett. **103**, 142604 (2013).
[32] T. Jacqmin, I. Carusotto, I. Sagnes, M. Abbarchi, D. D. Solnyshkov, G. Malpuech, E. Galopin, A. Lemaître, J. Bloch, and A. Amo, Phys. Rev. Lett. **112**, 116402 (2014).
[33] Y. Vlasov, W. M. J. Green, and F. Xia, Nat. Photonics **2**, 242 (2008).
[34] Q. Xu, B. Schmidt, S. Pradhan, and M. Lipson, Nature (London) **435**, 325 (2005).
[35] A. Melloni, F. Morichetti, C. Ferrari, and M. Martinelli, Opt. Lett. **33**, 2389 (2008).
[36] K. Fang, Z. Yu, and S. Fan, Phys. Rev. Lett. **108**, 153901 (2012).
[37] C. W. Gardiner and M. J. Collett, Phys. Rev. A **31**, 3761 (1985).
[38] R. B. Laughlin, Phys. Rev. B **23**, 5632 (1981).
[39] B. I. Halperin, Phys. Rev. B **25**, 2185 (1982).
[40] Y. Hatsugai, Phys. Rev. B **48**, 11851 (1993).
[41] D. Hofstadter, Phys. Rev. B **14**, 2239 (1976).
[42] D. J. Thouless, M. Kohmoto, M. P. Nightingale, and M. den Nijs, Phys. Rev. Lett. **49**, 405 (1982).
[43] Y. Vlasov and S. McNab, Opt. Express **12**, 1622 (2004).
[44] T. Barwicz, M. A. Popović, M. R. Watts, P. T. Rakich, E. P. Ippen, and H. I. Smith, J. Lightwave Technol. **24**, 2207 (2006).
[45] F. Xia, L. Sekaric, and Y. Vlasov, Nat. Photonics **1**, 65 (2007).
[46] C. Ferrari, F. Morichetti, and A. Melloni, J. Opt. Soc. Am. B **26**, 858 (2009).
[47] See Supplemental Material at http://link.aps.org/supplemental/10.1103/PhysRevLett.112.210405 for the effect of inhomogeneous effective magnetic fields can be tolerated.
[48] R. O. Umucalilar and I. Carusotto, Phys. Rev. Lett. **108**, 206809 (2012).
[49] M. Hafezi, M. D. Lukin, and J. M. Taylor, New J. Phys. **15**, 063001 (2013).